Journal of Cardiovascular Computed Tomography 13 (2019) 148–156

Contents lists available at ScienceDirect

Journal of Cardiovascular Computed Tomography

journal homepage: www.elsevier.com/locate/jcct

Research paper

Quantitative evaluation of non-ischemic dilated cardiomyopathy by late iodine enhancement using rapid kV switching dual-energy computed tomography: A feasibility study

Yasutoshi Ohta[a,*], Shinichiro Kitao[a], Hiroto Yunaga[a], Tomomi Watanabe[b], Natsuko Mukai—Yatagai[b], Junichi Kishimoto[c], Kazuhiro Yamamoto[b], Toshihide Ogawa[a]

[a] Division of Radiology, Department of Pathophysiological Therapeutic Science, Tottori University Faculty of Medicine, Yonago City, Tottori 683-8504, Japan
[b] Division of Molecular Medicine and Therapeutics, Department of Multidisciplinary Internal Medicine, Tottori University Faculty of Medicine, Yonago City, Tottori 683-8504, Japan
[c] Tottori University Hospital, Department of Clinical Radiology, Yonago City, Tottori 683-8504, Japan

ARTICLE INFO

Keywords:
Dual-energy
Computed tomography
Dilated cardiomyopathy
Myocardial delayed enhancement
Extracellular volume fraction

ABSTRACT

Objectives: The aim of this study was to evaluate the feasibility of myocardial iodine density and extracellular volume fraction (ECV) from delayed iodine density images using dual-energy computed tomography (DECT) for differentiation between non-ischemic dilated cardiomyopathy (NIDCM) patients and normal subjects.

Methods: Forty-six subjects were imaged, including 35 normal subjects and 11 patients with NIDCM. All subjects underwent myocardial delayed enhancement (MDE) imaging on rapid-kVp switching DECT. Global and segmental iodine density and ECV were calculated from MDE images. Histogram analysis was also performed. Receiver-operator characteristic (ROC) analysis was used to determine the cut-off value and diagnostic performances in differentiating NIDCM patients from normal subjects.

Results: Global iodine density and ECV were significantly higher in NIDCM compared with normal controls (iodine: 14.19 ± 3.90 vs. 10.69 ± 1.88 in 100 μg/cm^3, p = 0.015; ECV: 31.35 ± 2.53% vs. 26.62 ± 2.69%, p < 0.001). In histogram analyses, kurtosis was higher in NIDCM than in controls (0.47 ± 0.46 vs. 1.26 ± 0.88, p < 0.001). On segmental analysis, ECV showed higher values in NIDCM than in controls for all segments. ECV could differentiate between normal myocardium and NIDCM with 91.0% sensitivity and 86.0% specificity at a cut-off of 28.82% (area under the curve of ROC, 0.906). Iodine density could differentiate between normal myocardium and NIDCM with 91% sensitivity and 60% specificity at a cut-off of 11.18 (area under the curve of ROC, 0.812).

Conclusions: Iodine density and ECV values from DECT may provide indices offering high diagnostic accuracy for discriminating between NIDCM and normal myocardium.

1. Introduction

Myocardial fibrosis detection is important in the diagnosis and stratification of non-ischemic dilated cardiomyopathy (NIDCM). Cardiovascular magnetic resonance (CMR) enables the assessment of myocardial fibrosis using myocardial delayed enhancement (MDE), which can be used as a surrogate for replacement fibrosis.[1] Although MR-MDE is an accurate method for detecting myocardial replacement fibrosis and provides a prognostic index, sensitivity in the assessment of diffuse interstitial fibrosis is limited.[2,3] In recent years, extracellular volume fraction (ECV) measurement using MRI T1 mapping approach has been used to assess diffuse myocardial fibrosis.[4,5] Enlargement of the ECV by accumulation of collagen within the extracellular myocardial space is frequently observed in histological specimens of NIDCM, offers a useful indicator to differentiate diseased myocardium to normal myocardium,[6,7] and is predictive of all-cause mortality and heart failure events in NIDCM.[8]

ECV can also be computed using increments in CT number by subtracting non-contrast images from equilibrium phase images.[9–11] Generally, ECV measurements using a T1 mapping approach have been performed on three images from basal, mid, or apical slices on short-axis images or septum on four-chamber images, which do not cover the

* Corresponding author. Division of Radiology, Department of Pathophysiological Therapeutic Science, Tottori University School of Medicine, Yonago City, Tottori 683-8504, Japan.
E-mail address: ota.yasutoshi@ncvc.go.jp (Y. Ohta).

https://doi.org/10.1016/j.jcct.2018.10.028
Received 17 April 2018; Received in revised form 3 October 2018; Accepted 26 October 2018
Available online 29 October 2018

Abbreviations and acronyms list

CADS-RADS	coronary artery disease reporting and data system
CMR	cardiovascular magnetic resonance imaging
CT	computed tomography
CTA	computed tomography angiography
DECT	dual-energy computed tomography
ECV	extracellular volume fraction
GSI	gemstone spectral imaging
LGE	late gadolinium enhancement
LV	left ventricle
LVEF	left ventricular ejection fraction
MDE	myocardial delayed enhancement
NIDCM	non-ischemic cardiomyopathy
ROC	receiver operating characteristic curve
FWHM	full width at half maximum

entire left ventricular myocardium. However, this approach has issues in determining ECV cut-off values for differentiating between diseased and healthy myocardium when fibrotic changes to the myocardium are not homogeneous. In contrast, CT acquisition allows images of the whole left ventricle to be obtained in a single scan. ECV measurement using CT is also feasible and has been validated.[10–13] Moreover, dual-energy CT (DECT) using a rapid-kVp-switching approach that enables provision of iodine content in a voxel by density has been introduced. This allows for ECV measurement without pre-contrast images or with non-rigid image registration.[14]

The present study investigated the feasibility of applying myocardial iodine density and ECV from delayed iodine density images using DECT for differentiating between NIDCM and healthy myocardium in normal controls.

2. Methods

2.1. Study subjects

Seventy-six patients were referred to our radiological diagnostic department between October 2013 and February 2016 for cardiac CT imaging including coronary CT angiography (CCTA) and dual-energy delayed iodine enhancement, and CMR including MDE imaging performed as part of our institutional protocol to evaluate cardiomyopathies. Of these, 11 patients with NIDCM were retrospectively included in the study.

NIDCM was defined by the presence of: a) LV dilation and b) LV systolic dysfunction (left ventricular ejection fraction:LVEF < 55%) in the absence of c) hypertensive disease, d) valvular heart disease as evaluated on transthoracic echocardiography, or e) obstructive coronary artery disease (defined as ≥50% luminal stenosis on coronary CT angiography, i.e., CADS-RADS™ category ≥3), ischemic-pattern MDE on CMR, based on the classification from the European Society of Cardiology Working Group on Myocardial and Pericardial disease.[15,16] Endomyocardial biopsy was performed in 6 patients for clinical reasons and the results were considered compatible with dilated cardiomyopathy. Exclusion criteria were chronic renal dysfunction (estimated glomerular filtration rate < 30 ml/min/1.73 m^2), pregnancy, lactation, age < 40 years, or MR contraindications including implantable cardioverter defibrillators or incomplete CT or MR examination.

A total of 196 cases in our institutional cardiac CT database were examined between December 2014 and September 2015 for the purpose of excluding CAD. Of those, control CT-MDE data were extracted from 35 subjects matched for the following criteria: no major previous cardiovascular disease; normal findings on cardiac ultrasonography; normal findings on electrocardiogram; no history of diabetes mellitus, hypertension, and/or hyperlipidemia; and no significant coronary artery stenosis with CAD-RADS™ category 0 or 1.[16]

This retrospective study was approved by our institutional ethics committee in accordance with the Declaration of Helsinki, and the need to obtain informed consent was waived based on the retrospective nature of the analysis.

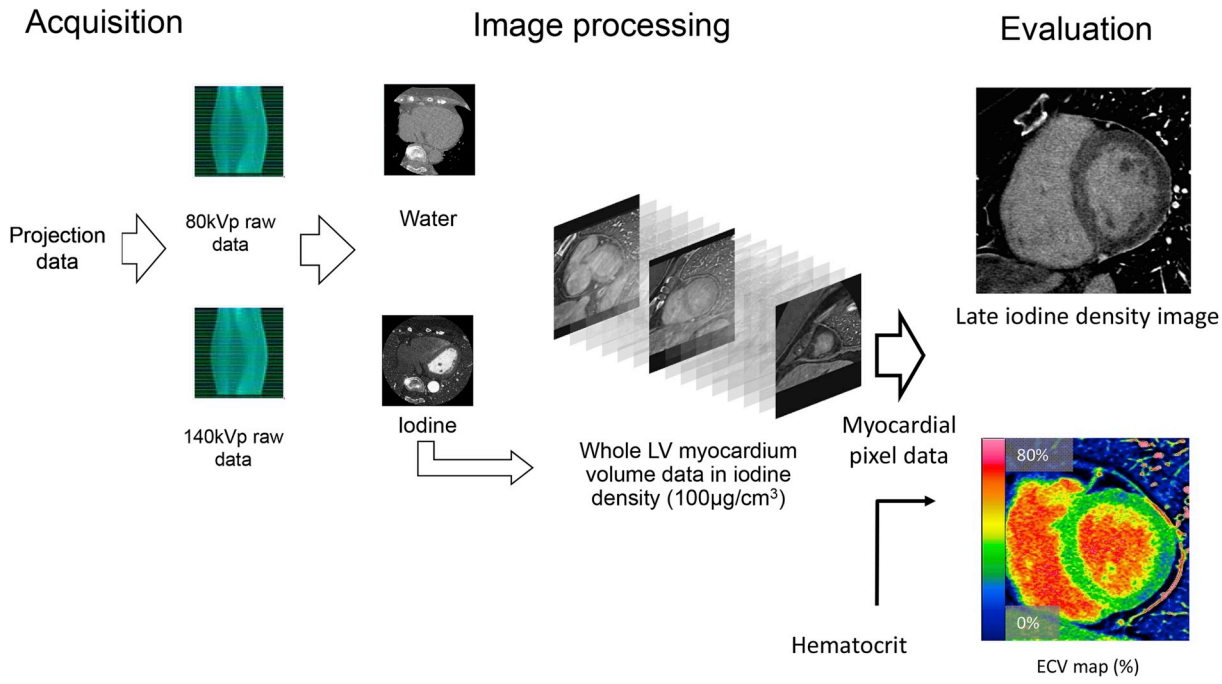

Fig. 1. Schematic flow chart from image acquisition to generation of iodine density and ECV maps using GSI.
ECV = extracellular volume fraction, GSI = gemstone spectral imaging.

Table 1
Baseline characteristics of subjects.

	Control (n = 35)	NIDCM (n = 11)	p Value
Age, years	71.53 ± 8.84	60.27 ± 9.22	**0.001**
Male	22 (65)	9 (82)	0.458
BMI, kg/m^2	22.62 ± 3.66	23.3 ± 2.91	0.58
Hypertension	0 (0)	7 (64)	< **0.001**
Diabetes mellitus	0 (0)	7 (64)	< **0.001**
Hyperlipidemia	0 (0)	4 (36)	**0.002**
EF, %	65.67 ± 5.97	33.75 ± 11.64	< **0.001**
LV wall thickness, mm	8.8 ± 1.35	9.76 ± 1.4	**0.047**
LVDd, mm	45.92 ± 5.64	58.21 ± 4.73	< **0.001**
Left atrium diameter, mm	36.25 ± 8.63	44.78 ± 5.92	**0.004**
E/A ratio	0.88 ± 0.25	1.34 ± 0.92	**0.012**
E/e' ratio	11.45 ± 3.74	15.94 ± 7.42	**0.011**
LV mass index, g/m^2	49.7 ± 10.39	61.49 ± 27.4	**0.04**
Estimated GFR, ml/min/1.73 m^2	79.41 ± 14.21	75.82 ± 23.76	0.55
Hematocrit, %	40.61 ± 4.17	44.06 ± 4.73	**0.026**
MR-MDE present	0 (0)	8 (73)	< **0.001**
CT-MDE present	0 (0)	8 (73)	< **0.001**

Values represent mean ± standard deviation or n (%). Comparisons between groups were made between normal control subjects and NIDCM patients. Significance relates to comparisons between control subjects and NIDCM patients (values of $p < 0.05$ were considered significant). Values in bold indicate significance. NIDCM = non-ischemic dilated cardiomyopathy, BMI = body mass index, EF = ejection fraction, LV = left ventricular, LVDd = left ventricular diastolic dimension, GFR = glomerular filtration ratio, LGE = late gadolinium enhancement, MDE = myocardial delayed enhancement.

2.2. CT protocol

All subjects received oral nitroglycerin 5 min before CT imaging. Subjects presenting with a heart rate ≥65 beats/min at 1 h before CT examination received oral beta-blocker (metoprolol, 20 mg). All CT images were acquired using single-source dual-energy 64-slice multidetector row CT (Discovery CT 750HD, Freedom Edition; GE Healthcare, Milwaukee, WI). Prior to MDE image acquisition, CCTA was performed upon intravenous infusion of 0.9 ml/kg of iopamidol (Iopamiron 370, 370 mgI/ml; Bayer Yakuhin, Osaka, Japan) over a period of 13 s. The routine CCTA protocol was as follows: tube voltage, 100 kVp or 120 kVp; prospective electrocardiogram gating, rotation time, 0.35 s. Immediately after CCTA, additional infusion of contrast medium at 0.5 ml/kg (maximum 100 ml) for 60 s was performed.[14]

CT-MDE acquisition was performed 7–8 min after CCTA using dual-energy scan (GSI cardiac; GE Healthcare) with the following parameters: tube voltage, 80–140 kVp rapid-kVp switching; tube current, 600 mA; rotation time, 0.35 s; prospective electrocardiogram gating: acquisition phase, mid-diastole; field of view, 180 × 180 mm, acquisition slice thickness, 0.625 mm; reconstruction slice thickness, 0.625 mm; adaptive statistical iterative reconstruction intensity, 80%.[17] This scanner allowed the use of tube currents from 375, 600 or 640 mA in dual-energy scan. As the 375 mA tube current might not guarantee image quality in large BMI patients, we selected a tube current of 600 mA for dual-energy acquisition. Dose length product was automatically recorded on the equipment.

2.3. Cardiac MRI

CMR was carried out on a 3.0-T scanner (Magnetom Skyra; Siemens Healthcare, Erlangen, Germany) with 18-channel phased array coil matrix (anterior and posterior). The cardiovascular MR protocol consisted of cine, T2-weighted short-tau inversion recovery, perfusion, and phase-sensitive inversion recovery imaging for MR-MDE using 0.15 mmol/kg of gadoterate meglumine (Magnescope; Fuji-Pharma, Tokyo, Japan). Cine imaging was performed with true fast imaging with steady-state free precession. MR-MDE imaging was performed 10 min after administration of contrast medium using phase sensitive inversion recovery: repetition time, 928 ms; echo time, 1.09 ms; flip angle, 40°; acquisition matrix, 144 × 192 pixels; and field of view, 250 × 340 mm. The interval between CT and CMR was 3 ± 7 days.

2.4. Image reconstruction and measurement

In iodine-density images, voxel values are expressed in mg/cm^3 [18]. Short-axis images of the LV myocardium using iodine-density images in 5-mm slices from base to apex were generated on a workstation (Advantage workstation, version 4.6; GE Healthcare). A schematic flow chart from projection data acquisition to image reconstruction is shown in Fig. 1.

The presence and pattern of both MR-MDE and CT-MDE images were evaluated by two independent specialists, a radiologist and a cardiologist, with 10 and 6 years of experience in cardiovascular imaging, respectively. If discrepancies existed between readers, a consensus was reached. To avoid recall bias in the qualitative evaluation, we evaluated MR-MDE images three months after the CT-MDE reading session.

The whole LV myocardial iodine density was extracted by placing the endocardium and epicardium contour using freely available Segment version 2.0 R4888 software (http://segment.heiberg.se).[19] Segmental and global iodine density and ECV were computed using American heart association (AHA) −16 segment. ECV was computed using the following equation. ECV(%) = (1-hematocrit) × (iodine density in myocardium)/(iodine density in LV blood pool) × 100.[14]

2.5. Quantitative analysis

Both iodine density and ECV were measured by segment base and whole LV myocardium. Distributions of iodine density or ECV within the myocardium were evaluated by histogram analysis. The resulting distributions were clearly mono-modal and were fitted using a Gaussian model to analyze distributions of iodine or ECV.

2.6. Statistical analysis

Categorical variables are expressed as proportions and were compared using the chi-square test. Continuous variables are expressed as mean ± standard deviation (SD) or median with interquartile range and were compared using the unpaired *t*-test or Mann-Whitney test. Correlations were evaluated using Person coefficients. Segmental and global differences in iodine density and ECV were compared between NIDCM and control groups. Parameters derived from histogram analysis were also compared between groups. Two-sided p-values less than 0.05 were considered statistically significant. Analysis was performed using SPSS Statistics version 23 software (IBM, Armonk, NY) and EZR[20] on R statistical computing (version 3.0.1, The R Foundation for Statistical Computing). Receiver operating characteristic curve (ROC) analysis to determine cut-off values for discriminating NIDCM myocardium from control myocardium was performed according to the DeLong method.[21] Diagnostic performances of iodine density and ECV for discriminating between NIDCM and normal myocardium were calculated. Histogram plots of iodine density extracted voxel-wise from the whole LV myocardium were generated to analyze the distribution of iodine density using a dedicated script written in MATLAB (The MathWorks Inc., Natick, MA) by one of the authors. The following histogram parameters were computed from histogram analysis: mean, mode, median, SD, kurtosis, and skewness. Gaussian curve fitting was also performed; and center, sigma, and full width at half maximum (FWHM) were calculated from the curve fitting data. In post-hoc sample size analyses setting alpha to 0.05, the powers of discriminating control and diseased groups for iodine, ECV and kurtosis were 81.9%, 100%, and 80.5%, respectively. The ROC powers for iodine and ECV were 91.6% and 99.9%, respectively.

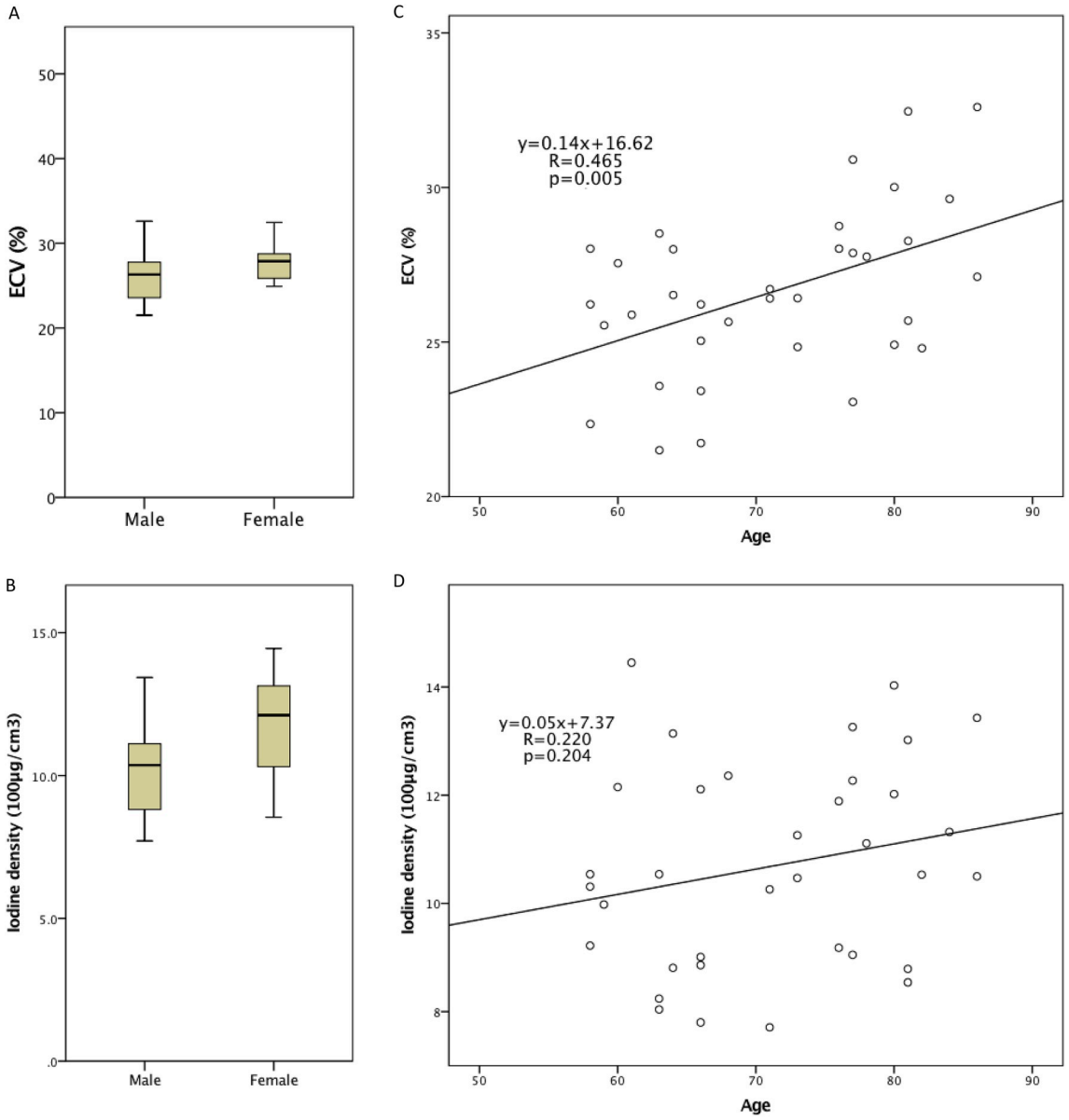

Fig. 2. ECV and iodine density in normal subjects.
Box-and-whisker plots show mean ECV (A) and iodine density (B) according to sex in normal subjects. (C) Global ECV is moderately associated with age. (D) No significant correlation is seen between iodine density and age. Abbreviations are as in Fig. 1.

3. Results

3.1. Subject characteristics

Subject characteristics and cardiac functions are presented in Table 1. In comparison with control subjects, patients with NIDCM showed reduced ejection fraction and increased left ventricular diastolic dimension (LVDd), left atrial diameter, E/A ratio, E/e' ratio, LV mass index, and hematocrit ($p < 0.05$). In NIDCM myocardium, hyperenhancement on CT-MDE images was observed in 8 patients (73%) as mid-wall enhancement that matched MR-MDE images.

3.2. Myocardial iodine density and ECV

Mean myocardial iodine density of control myocardium differed significantly between men and women (10.0 ± 1.5 vs. 11.8 ± 1.9, $p = 0.006$), but ECV did not (26.0 ± 2.7 vs. 27.8 ± 2.3, $p = 0.053$). ECV correlated with age ($r = 0.465$, $p = 0.005$), but not with iodine density ($r = 0.220$, $p = 0.204$) in control myocardium (Fig. 2). Both ECV and iodine density of each segment were significantly increased in the NIDCM group in all segments ($p \leq 0.026$), except for iodine density in segment 1 ($p = 0.058$) (Table 2). On global LV myocardium analysis, iodine density (14.19 ± 3.90 vs. 10.69 ± 1.88, in 100 µg/cm^3, $p = 0.015$) and ECV (31.35 ± 2.53% vs. 26.63 ± 2.69%, $p < 0.001$) were significantly higher in NIDCM patients than in control subjects (Table 2, Fig. 3).

3.3. Diagnostic performances

Results of ROC analysis with corresponding cut-off values for separate iodine density and ECV values in the differentiation control and NIDCM myocardium are demonstrated in Table 3 and Fig. 4. No significant difference was identified between areas under the ROC from iodine density (0.812) and ECV (0.906; $p = 0.177$). Using cut-off values from ROC analysis, iodine density and ECV showed the same sensitivity of 90.9%. ECV showed higher specificity than iodine density (85.7% vs. 60.0%).

Table 2
ECV and iodine density in NIDCM and controls.

AHA segment	ECV							Iodine density						
	NIDCM			Control			p value	NIDCM			Control			p value
1	29.76	±	4.66	26.36	±	3.10	0.008	13.59	±	4.65	10.55	±	1.77	0.058
2	38.36	±	3.89	31.88	±	3.49	< 0.001	17.37	±	4.83	12.78	±	2.15	**0.011**
3	37.72	±	4.20	31.86	±	3.37	< 0.001	17.03	±	4.52	12.76	±	2.08	**0.011**
4	30.64	±	3.98	27.07	±	4.43	0.021	13.83	±	3.67	10.89	±	2.46	**0.004**
5	30.78	±	4.94	23.28	±	4.18	< 0.001	13.76	±	3.58	9.37	±	2.28	< **0.001**
6	29.44	±	2.94	23.75	±	3.65	< 0.001	13.33	±	3.73	9.50	±	1.91	**0.007**
7	27.87	±	2.34	24.32	±	3.51	0.003	12.63	±	3.62	9.77	±	2.06	**0.002**
8	32.52	±	1.91	28.74	±	3.10	< 0.001	14.70	±	3.89	11.59	±	2.32	**0.002**
9	34.57	±	2.04	30.98	±	2.83	< 0.001	15.59	±	3.85	12.43	±	2.07	**0.001**
10	31.00	±	4.25	26.60	±	4.01	0.003	14.06	±	4.25	10.68	±	2.20	**0.026**
11	29.64	±	2.15	23.43	±	4.34	< 0.001	13.38	±	3.49	9.42	±	2.27	< **0.001**
12	28.27	±	3.14	23.21	±	3.47	< 0.001	12.84	±	3.74	9.32	±	1.98	**0.011**
13	28.90	±	2.98	25.17	±	3.69	0.004	13.06	±	3.64	10.10	±	2.01	**0.001**
14	31.50	±	2.72	28.79	±	2.51	0.004	14.29	±	4.23	11.58	±	2.05	**0.006**
15	31.26	±	2.74	27.26	±	3.08	< 0.001	14.17	±	4.06	10.94	±	2.01	**0.027**
16	28.78	±	2.99	23.75	±	3.58	< 0.001	13.02	±	3.60	9.56	±	2.12	**0.01**
17	31.87	±	4.21	26.24	±	3.52	< 0.001	14.53	±	4.79	10.50	±	1.89	**0.02**
Global	31.35	±	2.53	26.63	±	2.69	< 0.001	14.19	±	3.90	10.69	±	1.88	**0.015**

Values represent mean ± standard deviation. Comparisons between groups were made between normal control subjects and NIDCM patients. Significance relates to comparisons between control subjects and NIDCM patients (values of $p < 0.05$ were considered significant). Values in bold indicate significance. ECV = extracellular volume fraction, AHA = American Heart Association.

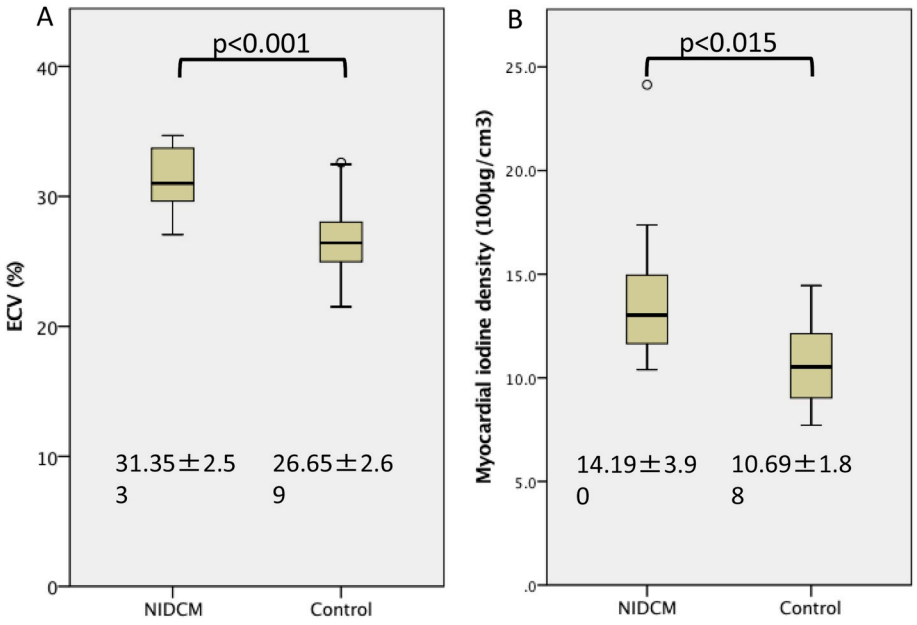

Fig. 3. Myocardial involvement in NIDCM patients as detected by ECV and iodine density quantification in whole LV myocardium as compared with control subjects.
Box plots show mean ECV (A) and iodine density (B) according to subject group. Horizontal bar indicates median, box denotes interquartile range, and whiskers refer to the range of values measured. NIDCM = non-ischemic dilated cardiomyopathy; other abbreviation as in Figs. 1 and 2.

Table 3
Results of cut off values on receiver-operator characteristic curve (ROC) analysis.

	Cut-off	AUC	Sensitivity (%)	Specificity (%)	PPV (%)	NPV (%)	Accuracy (%)
Iodine density, 100 µg/cm^3	11.2	0.812 (0.676–0.950)	90.9 (58.7–99.8)	60.0 (42.1–76.1)	41.7 (22.1–63.4)	95.5 (77.2–99.9)	67.4 (52.0–80.5)
ECV, %	28.8	0.906 (0.814–0.999)	90.9 (58.7–99.8)	85.7 (69.7–95.2)	66.7 (38.4–88.2)	96.8 (83.3–99.9)	87.0 (73.7–95.1)

Values in parentheses represent 95% confidence intervals. Cut-off values for differentiating NIDCM myocardium from normal myocardium were calculated from ROC curves. Diagnostic performances were calculated by applying the cut-off value. ROC = receiver-operator characteristic curve, AUC = area under the ROC curve, PPV = positive predictive value, NPV = negative predictive value.

3.4. Histogram analysis

Results of histogram and curve fitting analysis are shown in Table 4. Mean, mode, and median differed significantly between groups ($p \leq 0.04$). Kurtosis in NIDCM myocardium was higher compared to control myocardium on both iodine and ECV (1.26 ± 0.88 vs. 0.48 ± 0.46; $p < 0.001$). The skewness of distribution of iodine and ECV tended to be higher in NIDCM myocardium than in control myocardium (0.26 ± 0.22 vs. 0.18 ± 0.13), but the difference was not statistically significant ($p = 0.145$). From the curve-fitting results, the center of the curve was higher for NIDCM myocardium compared to control myocardium for both iodine density (13.94 ± 4.00 vs.

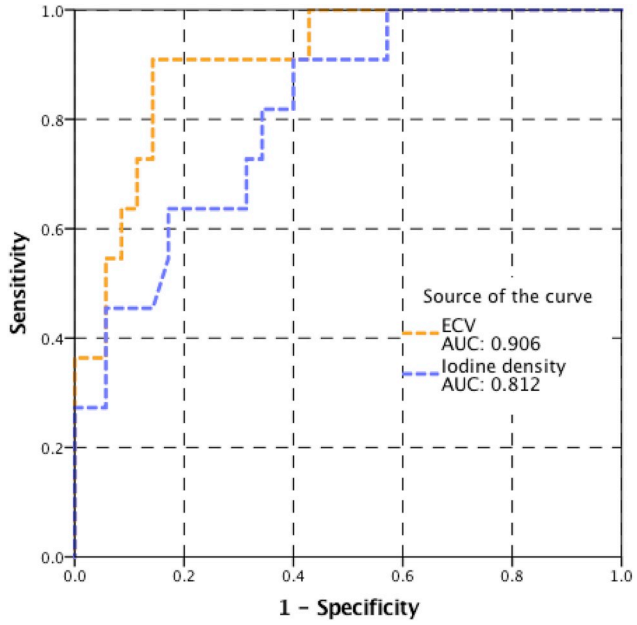

Fig. 4. ROC curves for differentiation of NIDCM and normal myocardium.
ROC = receiver-operator characteristic; other abbreviation as in Figs. 1 and 2.

10.82 ± 1.85, in 100μg/cm^3, p < 0.001) and ECV (30.94 ± 2.41% vs. 27.13 ± 3.28%, p < 0.001). The sigma and FWHM showed similar values (p = N.S). Representative cases and measurement results are demonstrated in Figs. 5 and 6. We did not measure the exact time needed for this quantitative analysis, but approximately 15–20 min was required.

The DLP for CT-MDE acquisition was 258.6 ± 14.3 mGy cm for both NIDCM and normal groups (p = 0.234).

4. Discussion

We demonstrated the difference of iodine density and ECV between control and NIDCM myocardium using iodine density and ECV from rapid kVp switching DECT. This may allow for discriminating normal and NIDCM myocardium with high diagnostic performance.

In our study, iodine density and ECV were elevated in all segments despite not all segments demonstrating detectable hyperenhancement on CT-MDE in NIDCM patients. No previous studies have demonstrated segment-based differences in ECV from the whole LV in NIDCM. We further demonstrated that histogram features of myocardial iodine density and ECV differed between the NIDCM and control groups. Our findings provide an new method for detecting NIDCM myocardium using CT-MDE following acquisition of CCTA.

In the diagnosis of NIDCM, ECV calculated from the T1 mapping approach has yielded high diagnostic performance in recent years.[7,22] MR-MDE has been used to identify myocardial fibrosis due to its high image contrast, especially when detecting replacement fibrosis. However, MR-MDE shows limited sensitivity for detecting diffuse interstitial fibrosis such as NIDCM. As the hyperenhancement in MR-MDE relies on signal differences between fibrosis and normal myocardium, signal differences are limited if the fibrosis is diffuse.[2]

Recently, ECV from T1 mapping has been used as an imaging biomarker of myocardial fibrosis with high diagnostic performance in differentiating NIDCM from control myocardium. In those studies, the diagnostic performances of iodine density and ECV using MR-MDE images were the same or higher than those of ECV using a T1 mapping approach (91.1% sensitivity; 62.1% specificity; AUC 0.8; ECV cut-off, 25.8%) or an AUC of 0.82–0.88 [7,22]. ECV cut-offs to best differentiate control and NIDCM myocardium differed between previous reports using the T1 mapping approach and our own results using iodine-density images. Besides inter-study differences in imaging modality and patient groups, CT measurements were performed for the whole LV myocardium in our study. However, some reports on ECV using a T1 mapping approach used only one or three slices (base, mid, and apex) to calculate myocardial ECV.[7,22,23] These differences help explain ECV differences between the two modalities and, therefore, this sampling limitation might affect the T1 values for myocardium in which the process of fibrosis is not homogeneous.[2] To obtain whole LV ECV, several T1 map acquisitions for both a pre-contrast T1 map and a post-contrast T1 map are performed with breath-holding. This does not necessitate the same position of the diaphragm for each breath hold, and cardiac dimensions are not exactly the same even if the acquisition interval is the same from the R-wave trigger. Non-rigid image registration is thus needed between pre- and post-contrast T1 maps.

ECV measurement using single-energy CT studies has been validated and demonstrated increased ECV in fibrotic myocardium such as with cardiac infarction or amyloidosis.[10–13] In a single-energy CT approach, the distribution of extracellular iodine contrast material was computed by subtracting the pre-contrast CT value from the post-contrast CT value. Under such circumstances, two processes as in the MRI T1 mapping approach are crucial: i) pre-contrast ECG-gated image acquisition for subtraction; and ii) accurate image registration using a non-

Table 4
Results of histogram and curve fitting analysis.

Iodine density	Control (n = 35)			NIDCM (n = 11)			p Value	ECV	Control (n = 35)			NIDCM (n = 11)			p Value
Histogram								Histogram							
Mean	11.01	±	1.94	14.21	±	4.09	**0.001**	Mean	27.6	±	3.34	31.53	±	2.52	**0.001**
Mode	10.62	±	1.97	13.8	±	3.91	**0.001**	Mode	26.62	±	3.81	30.68	±	3.14	**0.004**
Median	10.85	±	1.81	14	±	4.14	**0.001**	Median	27.21	±	3.06	31.02	±	2.77	**0.002**
SD	4.6	±	0.97	4.6	±	0.62	0.985	SD	11.66	±	2.47	10.64	±	2.36	0.256
Kurtosis	0.48	±	0.46	1.26	±	0.88	< **0.001**	Kurtosis	0.48	±	0.46	1.26	±	0.88	< **0.001**
Skewness	0.18	±	0.13	0.26	±	0.22	0.145	Skewness	0.18	±	0.13	0.26	±	0.22	0.145
Curve fitting								Curve fitting							
Center	10.82	±	1.85	13.94	±	4.00	**0.001**	Center	27.13	±	3.28	30.94	±	2.41	**0.001**
Sigma	4.45	±	0.84	4.36	±	0.68	0.748	Sigma	11.25	±	2.47	10.0	±	2.39	0.149
FWHM	3.78	±	0.72	3.71	±	0.57	0.748	FWHM	9.55	±	2.10	8.49	±	2.03	0.149

Values represent mean ± standard deviation. Comparison between groups was made between normal control subjects and NIDCM patients. Significance relates to comparisons between control subjects and NIDCM patients (p < 0.05) is considered Values in bold indicate significance. ECV = extracellular volume fraction, FWHM = full width at half maximum.

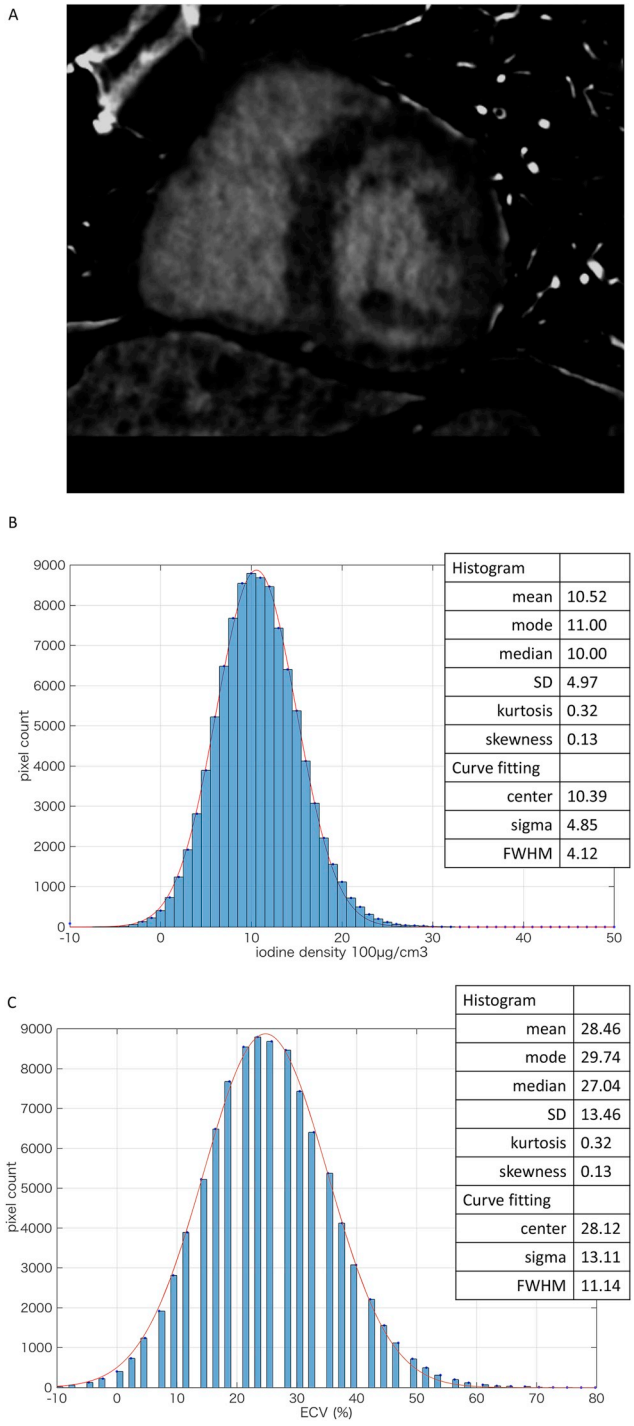

Fig. 5. ECV and iodine density quantification in control subject. A 70-year-old man, control subject. (A) CT-MDE in iodine-density image shows no apparent hyperenhancement in left ventricular myocardium.
Graphs show distributions of left ventricular myocardial iodine density (B) and ECV (C), which can be fitted using a Gaussian curve. Note that **bar graphs** indicate distributions of pixel counts in LV myocardium. **Red curves** indicate Gaussian fitting curves. SD = standard deviation, FWHM = full width at half maximum; other abbreviation as in Figs. 1 and 2. (For interpretation of the references to colour in this figure legend, the reader is referred to the Web version of this article.)

rigid approach. On the other hand, an iodine-density image approach offers some advantages: a) as iodine density shows the distribution of iodinated contrast agent in the extracellular space, pre-contrast CT for subtraction or image registration between two images is unnecessary and may actually cause inaccurate ECV measurements if misregistration occurs; and b) the source image is a myocardial delayed enhancement (MDE) image, enabling visual assessment of myocardium simultaneously with high diagnostic performance.[14,24] Iodine-density image-based measurement enables pixel-wise histogram analysis and demonstrated that kurtosis was significantly higher in the NIDCM group. This might be a new method to assess myocardial fibrosis, but verification requires larger clinical studies.

The advantages of ECV measurement by CT are simultaneous fast coronary artery assessment with a high negative predictive value that is crucial for the diagnosis of NICDM.[25] In recent years, dual-energy CT has been used for myocardial evaluation because it can provide parameters beyond the CT number.[26–29] In addition, CT-MDE from iodine-density images shows high diagnostic performance in differentiating ischemic and non-ischemic late enhancement patterns for identifying ischemic DCM.[30] Myocardial iodine density, ECV and distribution patterns from MDE images add useful information in the form of quantitative imaging biomarkers.

4.1. Limitations

Some limitations must be considered when interpreting the present results. First, this study included a relatively small number of NIDCM patients. Although post-hoc sample size analysis showed that a statistical discrimination power of 80% was satisfied, a larger cohort study would be preferable to make the diagnostic ability using this approach more robust. This study was also a retrospective study from a single center, and a larger, multicenter prospective study is required for further examination. Confirmation of the equivalence of multivendor dual-energy DECT systems may also be appropriate. Second, comparison with the histologic collagen fraction was not performed, because not all biopsy cases in this retrospective analysis underwent collagen staining for calculation of the collagen volume fraction. With the increasing use of MR-MDE for the evaluation of myocardial tissue characteristics, use of endomyocardial biopsy has decreased in routine clinical practice. Third, T1 mapping appears to be the best technique for evaluating NIDCM identified to date. For differentiating between normal and NIDCM myocardium, comparison not only with parameters derived from CT, but also Native T1 values and ECV by the CMR approach is desirable, However, during the study period, T1 mapping could not be performed because the T1 mapping sequence was not installed at the equipment in our institution. This issue should be further investigated.

5. Conclusions

The measurement of iodine density and ECV obtained from rapid kV switching single-source DECT seems clinically feasible for discriminating between NIDCM and healthy myocardium with high diagnostic accuracy and should be further evaluated.

Funding sources

This research did not receive any specific grant from funding agencies in the public, commercial, or not-for-profit sectors.

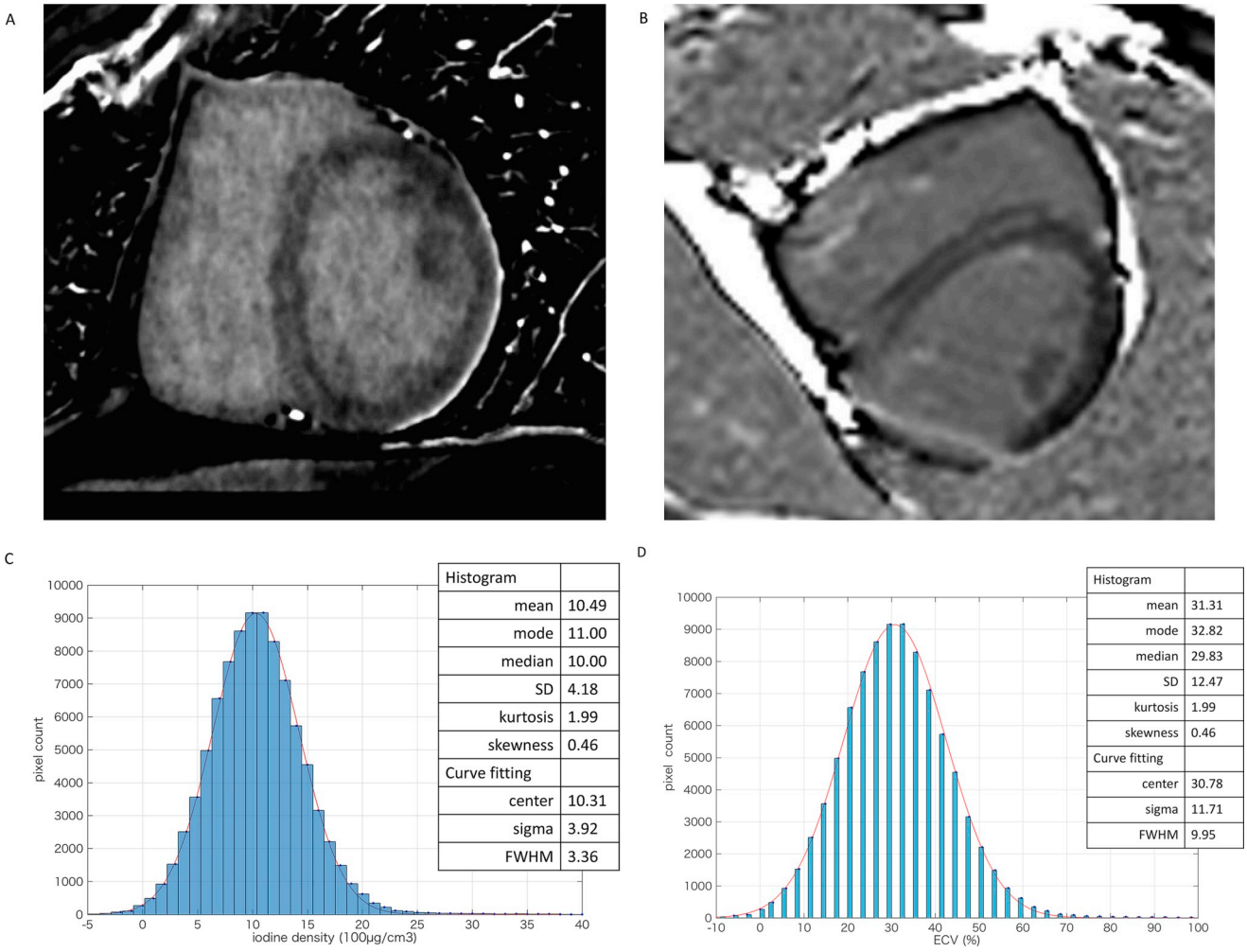

Fig. 6. ECV and iodine density quantification in NIDCM patient. A 70-year-old man with NIDCM. (A) CT-MDE image shows midwall hyperenhancement on the septum, as also identified on (B) MR-MDE.
Graphs show distributions of left ventricular myocardial iodine density (C) and ECV (D), which can be fitted using a Gaussian curve. Note that **bar graphs** indicate distributions of pixel counts in LV myocardium. **Red curves** indicate Gaussian fitting curves. MDE = myocardial delayed enhancement. Abbreviations as in Figs. 1, 2 and 5. (For interpretation of the references to colour in this figure legend, the reader is referred to the Web version of this article.)

Acknowledgements

None.

References

1. Ordovas KG, Higgins CB. Delayed contrast enhancement on MR images of myocardium: past, present, future. *Radiology.* 2011;261:358–374.
2. Mewton N, Liu CY, Croisille P, Bluemke D, Lima JA. Assessment of myocardial fibrosis with cardiovascular magnetic resonance. *J Am Coll Cardiol.* 2011;57:891–903.
3. Halliday BP, Gulati A, Ali A, et al. Association between midwall late gadolinium enhancement and sudden cardiac death in patients with dilated cardiomyopathy and mild and moderate left ventricular systolic dysfunction. *Circulation.* 2017;135:2106–2115.
4. Moon JC, Messroghli DR, Kellman P, et al. Myocardial T1 mapping and extracellular volume quantification: a society for cardiovascular magnetic resonance (SCMR) and CMR working group of the European society of cardiology consensus statement. *J Cardiovasc Magn Reson.* 2013;15:92.
5. White SK, Sado DM, Fontana M, et al. T1 mapping for myocardial extracellular volume measurement by CMR: bolus only versus primed infusion technique. *JACC Cardiovasc. Imaging.* 2013;6:955–962.
6. Brooks A, Schinde V, Bateman AC, Gallagher PJ. Interstitial fibrosis in the dilated non-ischaemic myocardium. *Heart.* 2003;89:1255–1256.
7. aus dem Siepen F, Buss SJ, Messroghli D, et al. T1 mapping in dilated cardiomyopathy with cardiac magnetic resonance: quantification of diffuse myocardial fibrosis and comparison with endomyocardial biopsy. *Eur Heart J Cardiovasc Imaging.* 2015;16:210–216.
8. Puntmann VO, Carr-White G, Jabbour A, et al. T1-Mapping and outcome in non-ischemic cardiomyopathy: all-cause mortality and heart failure. *JACC Cardiovasc. Imaging.* 2016;9:40–50.
9. Kurita Y, Kitagawa K, Kurobe Y, et al. Estimation of myocardial extracellular volume fraction with cardiac CT in subjects without clinical coronary artery disease: a feasibility study. *J Cardiovasc Comput Tomogr.* 2016;10:237–241.
10. Jablonowski R, Wilson MW, Do L, Hetts SW, Saeed M. Multidetector CT measurement of myocardial extracellular volume in acute patchy and contiguous infarction: validation with microscopic measurement. *Radiology.* 2015;274:370–378.
11. Bandula S, White SK, Flett AS, et al. Measurement of myocardial extracellular volume fraction by using equilibrium contrast-enhanced CT: validation against histologic findings. *Radiology.* 2013;269:396–403.
12. Nacif MS, Kawel N, Lee JJ, et al. Interstitial myocardial fibrosis assessed as extracellular volume fraction with low-radiation-dose cardiac CT. *Radiology.* 2012;264:876–883.
13. Treibel TA, Bandula S, Fontana M, et al. Extracellular volume quantification by dynamic equilibrium cardiac computed tomography in cardiac amyloidosis. *J Cardiovasc Comput Tomogr.* 2015;9:585–592.
14. Ohta Y, Kitao S, Watanabe T, et al. Measurement of myocardial extracellular volume fraction from iodine density images using single-source, dual-energy computed tomography: a feasibility study. *J Comput Assist Tomogr.* 2017;41:750–756.
15. Elliott P, Andersson B, Arbustini E, et al. Classification of the cardiomyopathies: a position statement from the European society of cardiology working group on myocardial and pericardial diseases. *Eur Heart J.* 2008;29:270–276.
16. Cury RC, Abbara S, Achenbach S, et al. CAD-RADS(TM) coronary artery disease - reporting and data system. An expert consensus document of the society of cardiovascular computed tomography (SCCT), the American college of radiology (ACR) and the north American society for cardiovascular imaging (NASCI). Endorsed by the American college of cardiology. *J Cardiovasc Comput Tomogr.* 2016;10:269–281.
17. Kishimoto J, Ohta Y, Kitao S, Watanabe T, Ogawa T. Image quality improvements using adaptive statistical iterative reconstruction for evaluating chronic myocardial infarction using iodine density images with spectral CT. *Int J Cardiovasc Imag.* 2018;34:633–639.

18. Alvarez RE, Macovski A. Energy-selective reconstructions in X-ray computerized tomography. *Phys Med Biol.* 1976;21:733–744.
19. Heiberg E, Sjogren J, Ugander M, Carlsson M, Engblom H, Arheden H. Design and validation of Segment–freely available software for cardiovascular image analysis. *BMC Med Imag.* 2010;10:1.
20. Kanda Y. Investigation of the freely available easy-to-use software 'EZR' for medical statistics. *Bone Marrow Transplant.* 2013;48:452–458.
21. DeLong ER, DeLong DM, Clarke-Pearson DL. Comparing the areas under two or more correlated receiver operating characteristic curves: a nonparametric approach. *Biometrics.* 1988;44:837–845.
22. Puntmann VO, Voigt T, Chen Z, et al. Native T1 mapping in differentiation of normal myocardium from diffuse disease in hypertrophic and dilated cardiomyopathy. *JACC Cardiovasc. Imaging.* 2013;6:475–484.
23. Hong YJ, Park CH, Kim YJ, et al. Extracellular volume fraction in dilated cardiomyopathy patients without obvious late gadolinium enhancement: comparison with healthy control subjects. *Int J Cardiovasc Imag.* 2015;31(Suppl 1):115–122.
24. Lee HJ, Im DJ, Youn JC, et al. Myocardial extracellular volume fraction with dual-energy equilibrium contrast-enhanced cardiac CT in nonischemic cardiomyopathy: a prospective comparison with cardiac MR imaging. *Radiology.* 2016;280:49–57.
25. Miller JM, Rochitte CE, Dewey M, et al. Diagnostic performance of coronary angiography by 64-row CT. *N Engl J Med.* 2008;359:2324–2336.
26. Wichmann JL, Bauer RW, Doss M, et al. Diagnostic accuracy of late iodine-enhancement dual-energy computed tomography for the detection of chronic myocardial infarction compared with late gadolinium-enhancement 3-T magnetic resonance imaging. *Invest Radiol.* 2013;48:851–856.
27. Deseive S, Bauer RW, Lehmann R, et al. Dual-energy computed tomography for the detection of late enhancement in reperfused chronic infarction: a comparison to magnetic resonance imaging and histopathology in a porcine model. *Invest Radiol.* 2011;46:450–456.
28. Kumar V, McElhanon KE, Min JK, et al. Non-contrast estimation of diffuse myocardial fibrosis with dual energy CT: a phantom study. *J Cardiovasc Comput Tomogr.* 2018;12:74–80.
29. Truong QA, Thai WE, Wai B, et al. Myocardial scar imaging by standard single-energy and dual-energy late enhancement CT: comparison with pathology and electronatomic map in an experimental chronic infarct porcine model. *J Cardiovasc Comput Tomogr.* 2015;9:313–320.
30. Ohta Y, Kitao S, Yunaga H, et al. Myocardial delayed enhancement CT for heart failure evaluation: comparison to MRI. *Radiology.* 2018;288:682–691.